



Influence of edge proximity on concrete breakout failure in post-installed RC columns foundation joints

Sara Cattaneo · Vinay Mahadik  · Giovacchino Genesio · Jan Hofmann

Received: 1 April 2023 / Accepted: 11 July 2023
© The Author(s) 2023

Abstract This paper discusses findings from an experimental program aimed at investigation of concrete breakout failure within the rebar end anchorage zone of reinforced concrete column-to-foundation joints, with columns located in proximity of foundation edge/s. A total of four tests on full scale column foundation joints are presented. In all specimens the column main reinforcement is anchored in the foundation using post-installed rebar technology. All connections are designed with the objective to trigger concrete breakout failure mode within the rebar end anchorage zone. Finite element analyses were used as a tool to design the specimens. The paper presents discussion of the test results within the framework of expectations outlaid during design of the test

specimens. The effects of bending compression from column on the concrete breakout capacity under influence of foundation edges is the specific focus of the present investigation. It is shown that the direction of application of load on the column largely determines the effect of bending compression from column on concrete breakout capacity. The test data presented in this paper offers the necessary benchmark data on concrete breakout behavior in the case of reinforced concrete column foundation joints under influence of foundation edges. This test data along with insights from finite element analyses is employed to explore and possibly identify necessary modifications to the current state-of-the-art consideration of concrete breakout capacity for reinforced concrete connections.

S. Cattaneo
Department of Architecture, Built Environment and Construction Engineering, Politecnico di Milano, 20133 Milan, Italy

S. Cattaneo
Construction Technologies Institute, Italian National Research Council (ITC-CNR), San Giuliano Milanese, MI, Italy

V. Mahadik (✉) · J. Hofmann
Institute of Construction Materials, University of Stuttgart, Pfaffenwaldring 4, 70569 Stuttgart, Germany
e-mail: vinay.mahadik@gmail.com;
vinay.mahadik@iwb.uni-stuttgart.de

G. Genesio
Hilti Entwicklungsgesellschaft mbH, Kaufering, Germany

Keywords Post installed rebar anchorage · Concrete breakout failure · Column foundation joints · Experiments · Edge influence

Abbreviations

CC	Concrete breakout failure associated with foundation concrete
CFJ	Column foundation joints
FE	Finite element
PI	Post installed (reinforcement anchorage)
RC	Reinforced concrete
MPII	Manufacturers product installation instruction



1 Introduction

Post-installed (PI) reinforcing bar (rebar) systems enable the installation of rebars into pre-drilled holes in hardened concrete using injected polymeric mortar. The experience developed in the last 30 years [1] made PI rebars a popular solution for the connection of reinforced concrete (RC) members. Connections with PI rebars are commonly employed for structural modifications or strengthening of existing structures. However, they can also be used in new structures to optimize the construction flow (e.g., avoiding steel bars sticking out from formworks to allow connection of additional reinforced concrete elements) or to solve issues such as missing rebars or misplacement of couplers. Common applications are connections between RC beams/slabs and columns/walls or RC columns/walls and foundations/slabs. Alternate technologies to realize connections of pre-cast RC members have also been extensively researched (typical examples in [2–5]). These techniques require sufficient reinforcement anchorage in the base (foundation) member to which the new reinforcement in the connecting member is spliced or connected using mechanical couplers within grouted sleeves. PI rebar technology offers possibility for realizing connections of rebars to the base members for applying such technologies in existing structures.

The main difference between cast-in (CI) place and PI reinforcing bars is the presence of bends/hooks (e.g., 90° standard bend) in the former case. Providing bends is not possible with PI reinforcing bars and the efficiency of the anchorage primarily depends on the mortar/adhesive and connection geometry. Often the connection geometry is crucial since small concrete cover and/or limited embedment length governs the critical failure modes (e.g., concrete breakout or splitting). These restrictions are common in beam-column joints and foundation/slab-column joints with column located close to an edge (investigated in this study).

The behavior of the two joints, is however different because of different boundary conditions. In the column–foundation joint the column axial load usually improves the capacity of the connection. In beam column joint, the concentrated joint shear forces resulting from connection mechanics are required to be mitigated [6, 7] to ensure the structural integrity of the joint region. On the other hand, typical RC column

foundation joints such complex mechanical situation of concentrated joint shear stresses [8, 9] is absent.

In case of PI reinforcing bar, the constraints on anchorage length based on the member dimensions and those on drilling procedures based on minimum cover requirement could potentially limit the practical applications. For these reasons, several studies [10–15] had been performed to assess the behaviour of RC connection using PI rebar technology. A comprehensive overview of these available studies in the context of possible load resistant mechanisms and the stress distribution within the connection subassembly was presented by Mahadik, et al. [8]. To compare different rebar end anchorage systems, one needs the specimen test matrix to span the range of parameters over which transition of failure modes specific to the rebar end anchorage zone occurs (i.e., bond failure, concrete breakout and steel yielding). Details of an extensive test program (13 full scale tests) on column foundation joints (CFJ) with specimens designed for specific failure modes using finite element (FE) analysis [16] have been presented by Mahadik et al. [17]. These studies [16, 17] provide the behavioural database (experimental and numerical), where transition in failure modes specific to rebar end anchorage zones is clearly manifested. Such data is vital for validation of assessment models for different possible failure modes related to rebar end anchorage zones in RC connections.

Recent development of system specific assessment procedures for bond resistance of PI rebar systems based on European Assessment Document (EAD) 332402 [18] issued by the European Organization of Technical Assessment (EOTA), provides the necessary window for consideration of realistic bond behavior in case of PI rebar end anchorage zones. Comprehensive design procedure for system specific design of rebar end anchorage zones in RC connections are made available in the Technical Report (TR) 069 [19]. The development of product specific assessment and design process for rebar end anchorage zones has been detailed by Mahadik et al. [1, 20]. The study presents a comparison of the system specific design method with other alternatively available methods for assessment of rebar end anchorage zone in the light of available test data.

According to the TR-069 [19] design procedure, concrete cone breakout failure based on provisions from EN 1992-4 [21] is one of the possible resisting



mechanism for rebar end anchorage zones. Over a certain range of (relatively small) straight anchorage lengths it has been shown experimentally that concrete breakout failure is crucial [1, 13, 15, 17, 22] and must be properly accounted [9, 14, 20, 23–25]. This has been shown to be true based on the straight anchorage length and is irrespective of whether an anchorage bend is available or not [1, 22]. Therefore, concrete breakout failure is considered as a possible mode of failure in the provisions of EOTA TR 069 [19]. It is highlighted here that the previous studies on concrete breakout failures in rebar end anchorage did not consider any influence of edge proximity. The objective of the present study is to investigate concrete breakout failure in rebar end anchorage zones considering the effect of edge proximity. For rebar end anchorages, such an investigation is required to be done systematically in combination of the compression force resulting from the bending moment in the column. Such comprehensive investigations which are largely missing (as per the knowledge of the authors') are presented in this paper and shall contribute towards better perspectives on concrete breakout failures in rebar end anchorage zones.

2 State-of-the-art concrete breakout model

The general expression for mean value of concrete breakout resistance for rebars in tension, is provided in (1) for uncracked concrete condition. A reduction factor of 0.7 applies when cracked state is assumed for the anchorage zone. Available studies on CFJ [8, 10, 13–15, 17, 24, 25], have demonstrated that in cases of concrete breakout failure of rebar end anchorage zone, the expression (1) for concrete breakout resistance provided in EN 1992-4 [21], provides a reasonably good capacity assessment. The available data is however limited to cases of column located away from influence of any edges.

$$N_{Rm,c} = N_{Rm,c}^0 \cdot \frac{A_{c,N}}{A_{c,N}^0} \cdot \psi_{s,N} \cdot \psi_{re,N} \cdot \psi_{ec,N} \cdot \psi_{m,N} \quad [\text{N}] \quad (1)$$

where $N_{Rm,c}^0 = 14.6 \cdot \sqrt{f_{cm}} \cdot h_{ef}^{1.5}$...is the basic breakout resistance of a single bonded anchor in non-

cracked concrete [N]. f_{cm} is mean cylinder strength of concrete (MPa). h_{ef} is the straight anchorage length (mm). $A_{c,N}^0 = (2c_{cr,N})^2 = (s_{cr,N})^2$ is the reference projected area of a single anchor (rebar), with $s_{cr,N} = 2c_{cr,N} = 3h_{ef}$. $A_{c,N}$ is the projected area of group of anchors (rebars). $\psi_{s,N}$ is the reduction factor to account for the influence of vicinity of edge on stress distribution. $\psi_{re,N}$ is the shell spalling factor to account for dense reinforcement. Not applicable (= 1) for discussions in the scope of this paper. $\psi_{ec,N}$ is a reduction factor to account for the eccentricity of loading w.r.t. the anchor arrangement. Not applicable (= 1) for discussions in the scope of this paper. $\psi_{m,N} = 2.0 - \frac{z}{1.5h_{ef}} \geq 1$ is an increase factor to account for beneficial effect of moment loading (bending compression) on the concrete breakout resistance. = 1 under influence of edges. = 1 when bending is accompanied with axial tension. = 1 when $z \geq 1.5 \cdot h_{ef}$. z is the internal lever arm between the tension and compression forces

If the column is located near a foundation edge, a requirement of which may arise in real construction situations, the development of a full concrete cone is restricted by the presence of edges. In such situation, the reducing effect of the edge on the concrete cone breakout resistance is considered through a combination of three factors: (i) the projected area $A_{c,N}$ is reduced depending on edge presence w.r.t. the anchored rebars, (ii) reduction factor $\psi_{s,N}$ applies in case of edge vicinity to account for the disturbance of stresses and (iii) the beneficial effect of bending compression through factor $\psi_{m,N}$ is not applicable (= 1). The consideration of the effects of edge presence on concrete breakout resistance through the parameters $A_{c,N}$ and $\psi_{s,N}$ is done in a harmonious and integrated manner [26, 27]. In a way the two parameters are complementary to one another in assessment of the breakout resistance. The effect of bending compression through the factor $\psi_{m,N}$ is accounted for in an independent manner. Such effect of bending compression, although accounted for in EN 1992-4 [21], is not considered in the provisions of ACI 318 [28]. It has been shown [1, 17, 20] that a consideration of effects of bending compression on concrete breakout resistance is required for a realistic assessment of test data showing concrete breakout failure.

3 Research motivation and objective

Sufficient test and numerical database are available for consideration of effect of bending compression on concrete breakout resistance in case when the anchorage zone is away from any influence of edges. The database on effects of bending compression on concrete breakout resistance under the influence of edge vicinity is largely absent [8, 13–15, 17]. Consequently, the factor ψ_{mN} is conservatively assumed to be = 1. The objective of this paper is to investigate possible effects of bending compression on concrete breakout resistance of anchorage zone under influence from edges in vicinity. CFJ with column placed near the foundation edge are considered. A special application case in which the column surface at the edge is flushed with the foundation edge surface is considered, since it is most critical for possible influences of edge presence on concrete breakout resistance. FE studies are conducted for designing suitable specimens in a benchmark test program. In this process, the direction of the applied horizontal load on the column is concluded to be the controlling parameter. Test specimens (total of 4 full scale column foundation joints) designed based on FE analyses are subjected to monotonically increasing column horizontal displacement to evaluate the actual response. The paper discusses the details of the test procedure and presents the findings. Combined insights from the test data and FE studies are discussed.

4 Test program: design of specimens

4.1 FE modelling approach and validation

FE modelling and analysis was used to design specimens. The FE approach (modelling procedure and solvers) used in previous studies [8, 16, 17] has been adopted. The FE model was generated using the pre-processing interface of commercially available software FEMAP [29]. The program MASA [30] was used as a FE solver, the results from which were visualized in post-processing using FEMAP [29]. Concrete was modelled using 4 node tetrahedral elements with 3 degrees of freedom at each node. The microplane model with relaxed kinematic constraints [31] was used as a material law. The input stress–strain curves for concrete corresponding to the

material properties used in the analyses are shown in Fig. 1a. The main reinforcement bars of the column, with end anchorage in the foundation were modelled using hexahedral elements with 3 degrees of freedom at each node. Von-Mises based criteria was used for defining the nonlinear behavior expressed using a trilinear assumption as shown in Fig. 1b. A contact layer with hexahedral elements was modelled between the rebars and concrete, within which bar elements were used to define the multi-linear bond-slip relation governing the contact. The bond slip law corresponding to the post-installed rebar anchorage system used in the present study was obtained based on the confined tests on single post installed rebars showing pure bond pull out failure.

Since the focus of the present study is the simulation of concrete breakout failure, the specimens with post-installed rebar anchorage using a high strength PI rebar system failing with concrete breakout as the dominant resistant mechanism were considered. The PI specimens with an anchorage length of 250 mm (CFJ-PI-4D25-L250, monotonic: MON and cyclic: CYC [17]) showed concrete breakout as the dominant failure mode in the experiments. A comparison of test results with the FE simulation using a half model from the previous study (FE-Half) is reproduced in Fig. 2. It is noted that in the FE analysis only monotonically increasing displacement was applied.

The present study aims at investigating concrete breakout failure in the vicinity of edges. Therefore, depending on the direction of the load on the column, in some cases, it would not be possible to take advantage of symmetry in the FE modelling. Hence, a full FE model is considered in contrast to half models used in the previous study [17].

4.2 FE studies for specimen design

The CFJ-PI-4D25-L250 specimen [17] considered for validation, serve as a reference specimen (no edge influence) in this study. All specimens considered in the present paper have the same column configuration, CFJ-4D25 (300 × 300 mm column with 4-25 mm bars) with column main bars anchored using the same post-installed rebar system (having confined bond strength in the range of 30–35 MPa) used in the previous study [17] with anchorage length of 250 mm. For CFJ, two edge proximity scenarios are practically possible: (i) Side situation—one edge in proximity and



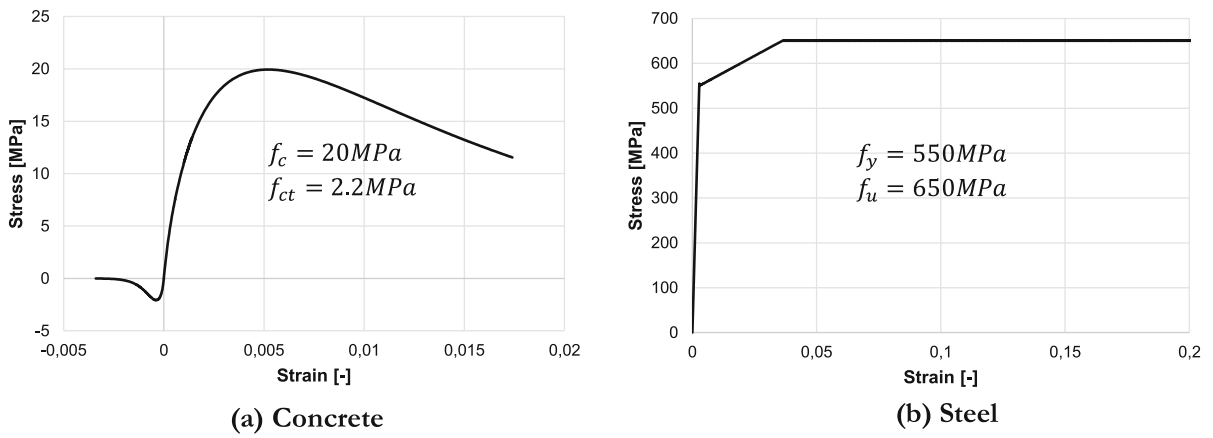
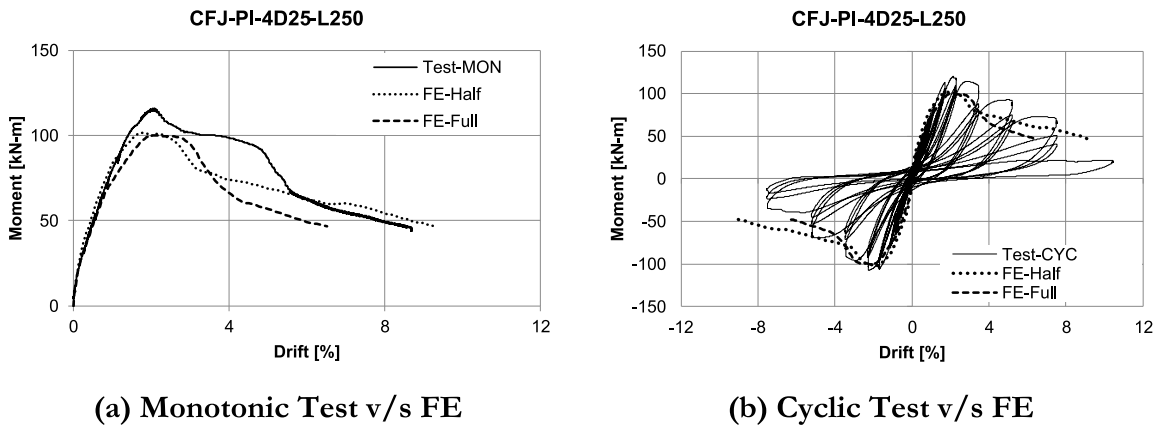
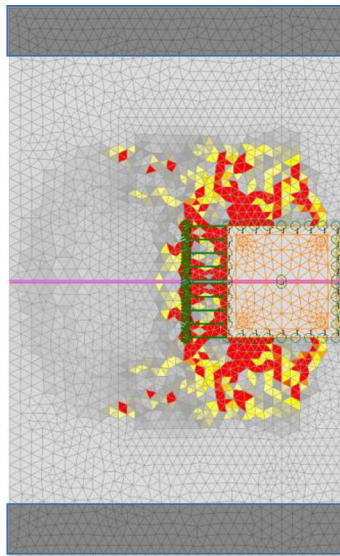


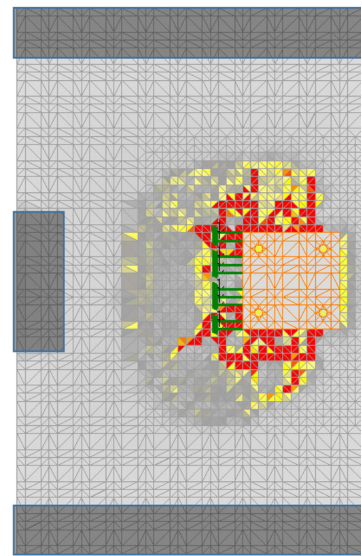
Fig. 1 Material definition used in FE analysis



(c) Crack Pattern: Test



(d) Crack Pattern: FE-Half



(e) Crack Pattern: FE-Full

Fig. 2 Comparison of FE results (old: FE-Half [17] and new: FE Full) with test data under validation

(ii) Corner situation—two adjacent edges in proximity. Depending on the direction of column horizontal load relative to the orientation of the foundation edge, distinctly different concrete breakout scenarios result. These differences are manifested as truncated projected concrete cone areas as schematically represented in Fig. 3, where the plane containing the tension rebars and the projected concrete cone breakout area on the foundation surface is shown for each case. A system of nomenclature used in this study for identifying all relevant parameters is also explained in Fig. 3. The term edge offset, defined as the distance of the foundation edge from the face of the column is used to define the edge distance. In case of the corner situation, equal edge offsets are considered in the present study.

To evaluate the effects of edge influence on concrete breakout resistance, it is intuitive that the case with edge offset equal to zero offers the worst-case influence. To this end, in FE analyses, the column placed in a way that the face of the column and foundation is flushed together is considered i.e. $X = 0$ in Fig. 3. This corresponds to an edge distance of

50 mm for the outermost column main rebar. The 5 different edge scenarios in Fig. 3 for $X = 0$ were considered in the FE analytical matrix in order to get insights into the possible response. The resulting proposal for benchmark testing is discussed.

The boundary conditions used in the FE models compatible with the recommendations [8] suggested for simulation of mechanical state in case of column foundation joint for the 5 cases are presented in Fig. 4a. Horizontal restraints were applied to the vertical edges of foundation transverse to the loading direction in a manner that they do not interfere with the anchorage zone behavior. Vertical restraint was applied on the top surface of the foundation along its edges as shown schematically in Fig. 4a. Monotonically increasing horizontal displacements in direction as required for each case were applied to the column at the top. It is noted that the column axial load is not applied in any case, because zero column axial load presents the most critical situation [1, 17, 20] for concrete breakout failure in the foundation. Column axial load equal to zero, facilitates the triggering of the

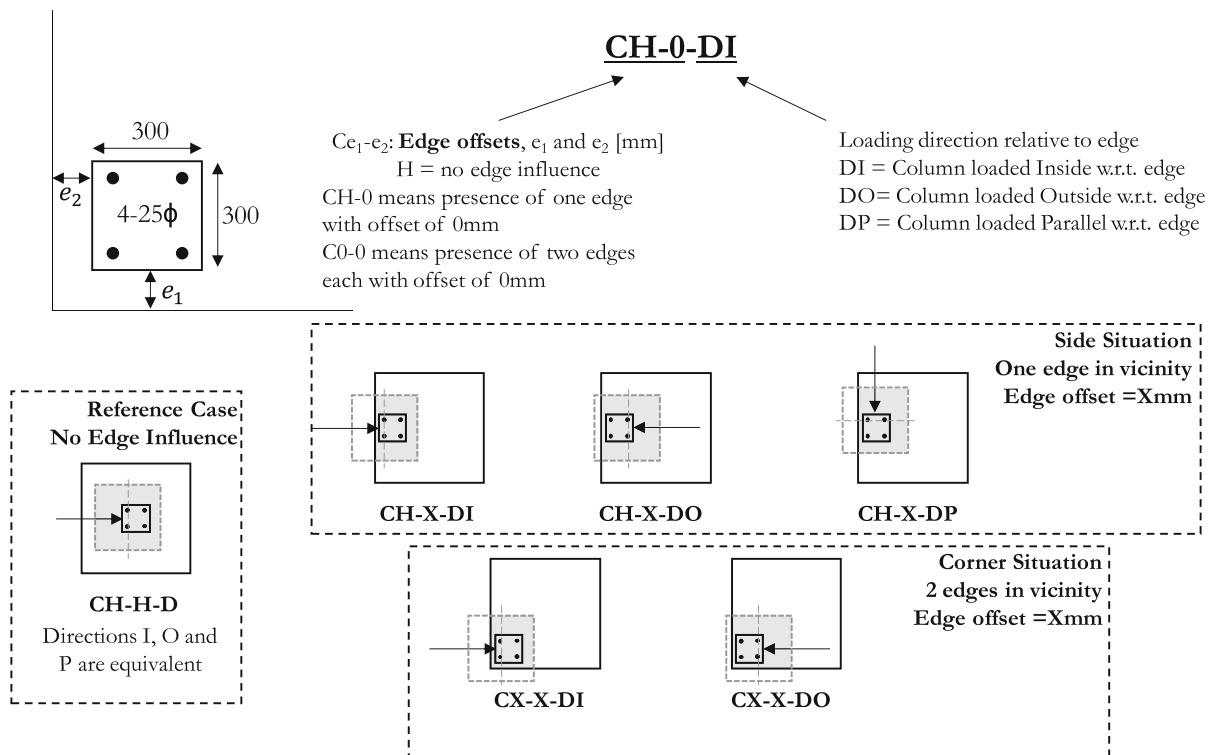
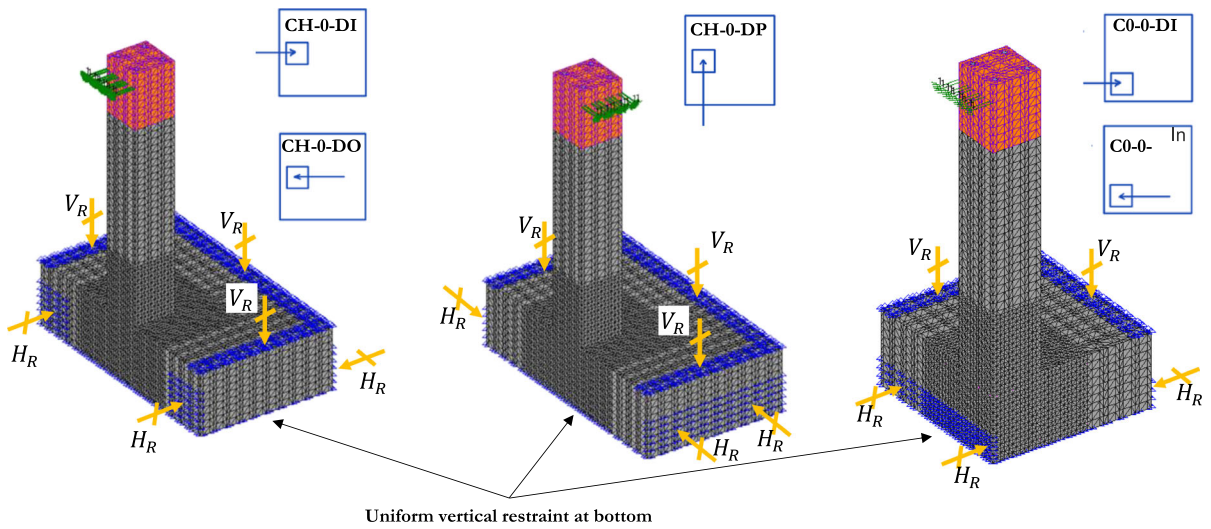
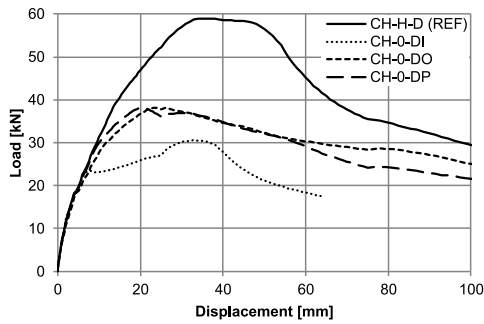


Fig. 3 Schematic representation of varying parameters and nomenclature used in the present study

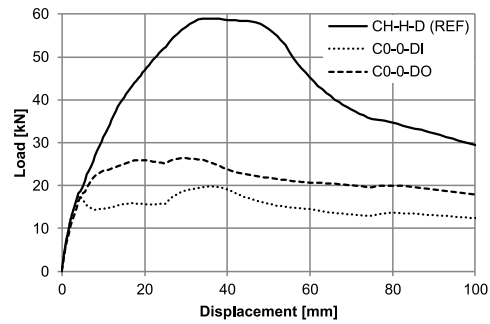




(a) Boundary Conditions



(b) Side Situation



(c) Corner Situation

Fig. 4 Boundary conditions in FE analysis and load displacement results

concrete breakout failure which is the subject in this paper.

The load displacement curves obtained from FE analyses for the 3 cases of “Side Situation” and two cases of “Corner Situation” are compared with the reference case (no edge influence) in Fig. 4b, c respectively. Concrete breakout failure was observed in all analyses. The effect of influence from edges is clearly seen to reduce the concrete breakout resistance in all cases when compared to the reference case with no edge influence. The presence of foundation edge in vicinity of the rebar end anchorage zone leads to truncation of concrete breakout cone, thereby reducing the effective rebar tension force at which concrete breakout failure occurs. A particularly distinct response was observed for cases in which the column

was loaded towards the inside w.r.t. the edge (CH-0-DI and C0-0-DI) in comparison to all other cases. The load displacement response showed two well defined peaks. The first peak was caused by formation of concrete breakout cracks on the foundation edge behind the column. Following the drop after the first peak, the load capacity increased because of the stabilization of strut offered by the bending compression force.

In order to provide a perspective on the influence of bending compression on concrete breakout capacity based on FE results, the expression (1) is rearranged as shown in (2) in order to evaluate the factor $\psi_{m,N}$ based on the rebar tension force evaluated in the FE analyses. A summary of FE results is provided in Table 1. The value of $\psi_{m,N}$ evaluated from each analysis is

presented. Furthermore, the applicable value of $\psi_{m,N}$ as per provisions of EN 1992-4 [21] is also included for comparison.

$$\psi_{m,N} = \frac{N_{R,cc}}{N_{Rm,c}^0 \cdot \frac{A_{c,N}}{A_{c,N}^0} \cdot \psi_{s,N} \cdot \psi_{re,N} \cdot \psi_{ec,N}} \quad (2)$$

where $N_{R,cc}$ is the rebar tension force evaluated in FE analyses for concrete breakout failure mode (N). All other terms are as defined in (1).

As discussed earlier and pointed out in Table 1, EN-1992-4 [21] recommends a value of $\psi_{m,N} = 1.0$ for all cases with edge proximity. The value of $\psi_{m,N}$ from FE evaluation in all cases with edge proximity was found to be greater than 1. Furthermore, for all cases with edge proximity except for CH-0-DO, the value of $\psi_{m,N}$ from FE analysis was found to be higher than the value of $\psi_{m,N}$ recommended by EN-1992-4 [21] for the case with no-edge influence (CH-H-D (REF)). To confirm the correctness of these observations, benchmark test program involving monotonic tests on 4 full scale column foundation joints was taken up. The cases CH-0-DI, CH-0-DO, CH-0-DP and C0-0-DO were tested.

The details of the experimental program are provided in the following section. The collective insights from FE analysis and experimental findings is discussed later in Fig. 7. In these discussions the influence of bending compression on concrete breakout resistance for PI rebar end anchorages under the influence of foundation edges is clearly identified.

5 Test procedure and results

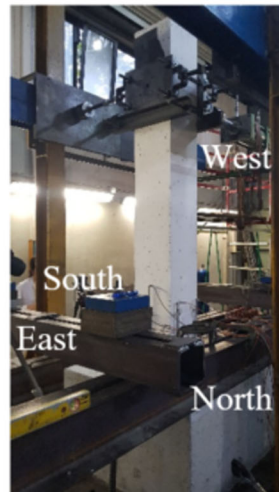
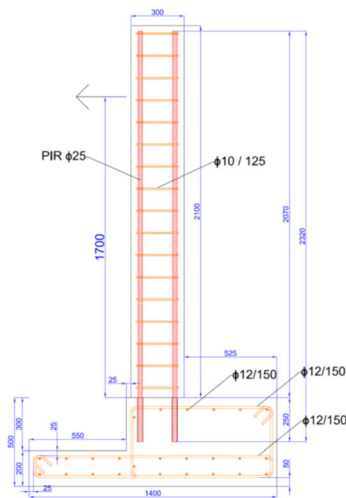
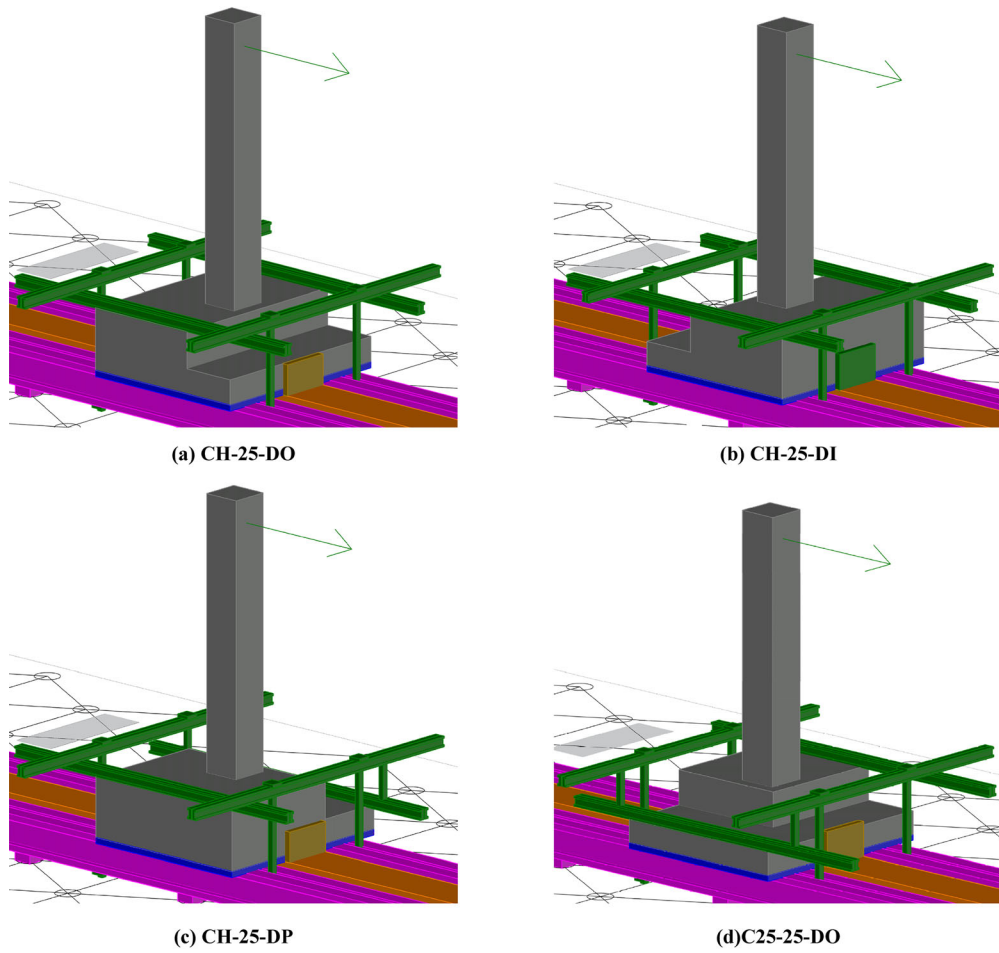
5.1 Preparation of specimens

The test set-up was designed to simulate the boundary conditions as schematically shown in Fig. 4a. The shape of the geometries used in the FE model are such that, restraining the torsional movements of the specimen about the vertical axis is practically challenging, and may likely cause localized damage at the restrained location due to rigid body rotation of the dissymmetrical specimens. This is particularly critical for specimen with loading parallel to the edge and the corner specimen. In order to solve this issue, the bottom of the foundation block was kept 1400 mm × 1400 mm for all the specimens, with the column (300mm×300mm section) located at the geometric center of the plan. In order to realize the required foundation edges, step was introduced in the foundation block. The total height of the foundation block and the height of the step was kept 500 mm and 200 mm respectively for all the specimens (with two sides for the corner specimen). This provided an edge depth of 300 mm along the anchorage length of 250 mm in all cases. The resulting shapes of the specimens can be seen in Fig. 5. A photograph of the test set up and the specimen geometry for case CH25-DP is also shown. The step facilitated the application of boundary conditions (see Fig. 5) representative of that used in FE simulations (see Fig. 4a). For all specimens, the foundation slab was reinforced with 12 mm rebars as top and bottom surface reinforcement provided in form of hoops, spaced at 150 mm in both

Table 1 Summary of FE results

ID	Peak colm. load (kN)	Displacement at peak load (mm)	Peak interface moment (kN m)	Rebar tension force (kN)	$\psi_{m,N}$ as per (2) (–)	Applicable $\psi_{m,N}$ [21] (–)
CH-H-D (REF)	59.02	36.0	100.33	445.93	1.36	1.40
CH-0-DI	30.52	33.0	51.89	230.60	1.68	1.00
CH-0-DO	38.13	23.5	64.83	288.12	1.18	1.00
CH-0-DP	38.05	20.0	64.69	287.50	1.81	1.00
C0-0-DI	19.73	36.0	33.54	149.06	1.65	1.00
C0-0-DO	26.35	30.0	44.79	199.07	1.50	1.00





(e) Specimen detail and test set up photograph for CH-25-DP

Fig. 5 Schematic representation of Specimen shapes, boundary and loading conditions in tests

directions. 10 mm stirrups spaced at 125 mm were used as transverse reinforcement for all columns. Achieving the zero edge offset as used in the FE analysis was practically challenging given the location of foundation reinforcement at edge and practical cover requirements, particularly for the case of column in the corner. An edge offset of 25 mm was the minimum practically possible dimension for this case. Hence in all the four specimens the offset (parameter X in Fig. 3) was made 25 mm.

The casting of specimens was made in two stages. In the first stage, the foundations were cast using the same concrete batch at a precast concrete manufacturer. At foundation concrete age of about seven weeks, the longitudinal bars of columns were post-installed. Prior to installation, all longitudinal rebars were prepared in laboratory with two strain gauges (installed on diametrically opposite points on the circumference of the rebar at a distance of 275 mm from the anchored end), to measure the rebar strains at the column section just outside the foundation/column interface.

The rebars were installed according to Manufacturer Product Installation Instruction (MPII) of the adhesive. For installation of the 25 mm rebars, borehole of diameter 32 mm were drilled at the desired location in each foundation. The holes were cleaned using passing of compressed air and brushing (2 + 2 + 2) as recommended in MPII. The anchorage length (borehole depth) was 250 mm in all tests. The holes were filled with post installation adhesive in sufficient amount using the tools available from the manufacturer which avoided any air gaps for deep anchorage lengths. The longitudinal bars were inserted in an orientation that resulted in all strain gauges positioned in the same direction with respect to the edge of the specimen. The bars were maintained in vertical position with wood wedges. After 18 h of curing, stirrups were fixed to the rebars and column formworks were prepared. In the second stage, the columns were cast about 24 h after installation of the rebars.

Concrete cubes (side 150 mm) and cylinder (height 300 mm, diameter 150 mm) were cast to evaluate the compression and tensile strength respectively for the concrete batches. The average compressive strengths were 22.4 MPa and 29.6 MPa for the foundation and for the columns respectively. The average splitting tensile strength of the foundation at the time of testing was 1.5 MPa. Steel B500B was employed for the column main reinforcement. The yield and ultimate

strength of the PI rebars were 564.2 MPa and 656.8 MPa respectively.

5.2 Test set-up, instrumentation and loading

The tests were performed using a test set up arrangement as shown in Fig. 5e. The specimens were positioned so that the vertical axis of the column intersected the horizontal axis of the actuator. Horizontal and vertical restraints as shown in Fig. 5 were applied using an arrangement of steel beams tied to the strong floor using tie rods. The actuator was connected to the column through a fixture attached to the column at a distance of 1.7 m above the top surface of the foundation. The tests were displacement controlled.

A total of 18 LVDTs were used to measure the specimen response of each test. For each specimen the arrangement of the instruments (see Fig. 6) was done for three measuring objectives: (i) measurement of column rotation for the critical section along three planes in the loading direction using 3 pairs of instruments labelled as R (in green) (ii) measurement of splitting crack widths on the foundation surface and edge depending on the expected occurrence of cracks based on FE results using instruments labelled as S (in red) and (iii) measurement of uplift of the foundation top surface w.r.t the test floor using instruments labelled as U (in blue). Each instrument is identified based on the objective of the measurements (R, S or U and the relative position (i.e. N = north; S = south..., D = diagonal) plus an additional number in case of multiple measurements if applicable. In addition to the displacement measurements, the load and displacement of the actuator and eight strain gauges' (two on each longitudinal bar of the column) readings were recorded with HBM Spider 8 data acquisition system.

5.3 Combined insights from tests and FE analysis

The experimental results in all cases were found to be comparable with the FE analyses used to design the test program. Behavior of each specimen based on the combined insights from FE analysis and test is discussed in this section. It is noted that the discussions presented in this section considers comparison of response of specimens tested with an edge offset = 25 mm with FE analyses conducted using an edge offset of 0 mm.



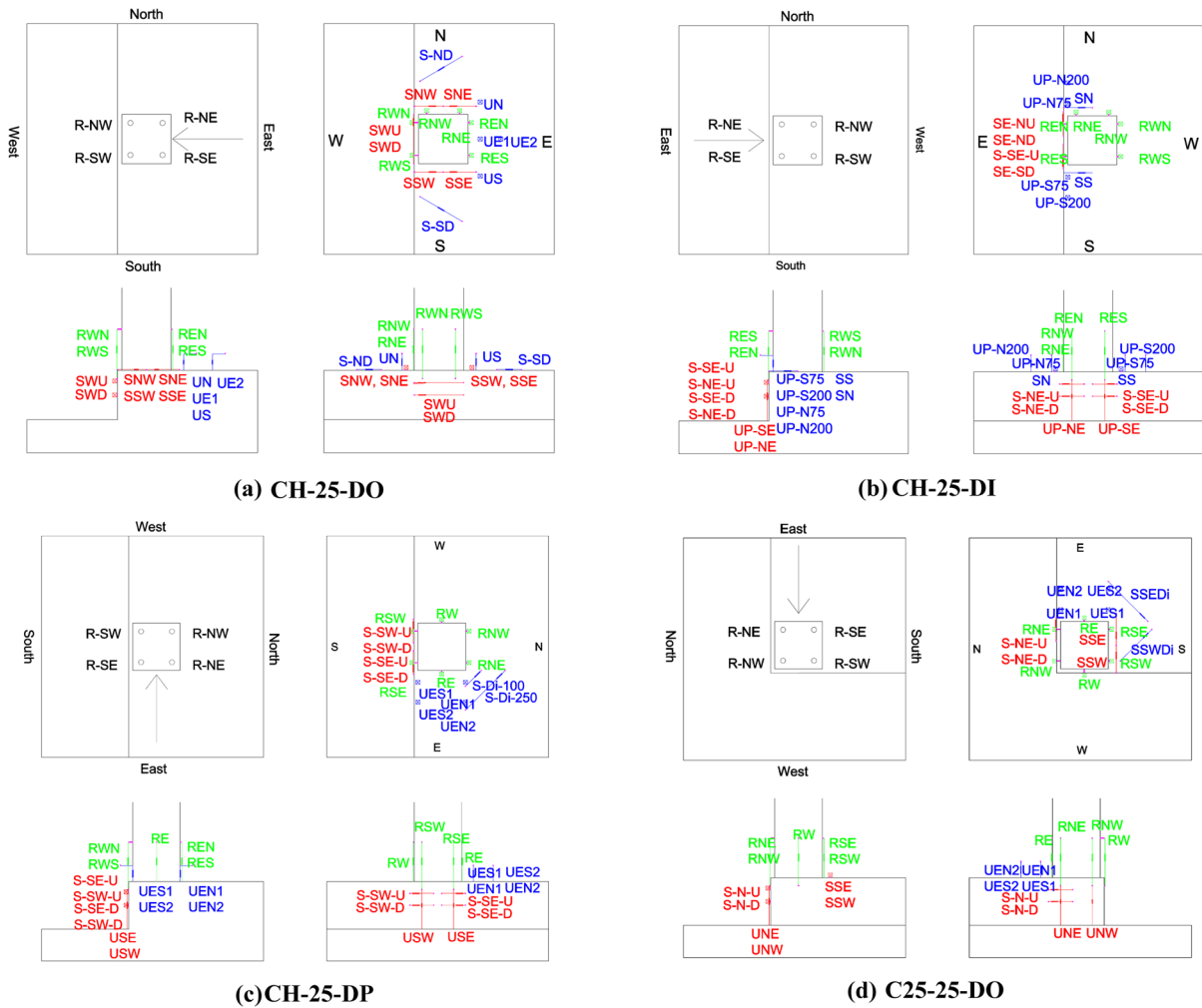


Fig. 6 Schematic arrangement of instrumentation for measuring displacements and crack widths

A summary of all test results relevant for the discussion is presented in Table 2. The peak load, displacement at the peak load, total tension force in column main rebars calculated from peak bending moment (M) and also from strain gauges measurements (SG) are presented. The ratio of peak tensile stress in the rebar and the design yield strength of rebars show that yielding of rebars did not occur in any of the tests. All specimens exhibited clear concrete cone (CC) failure.

Each specimen is characterized with a distinct fracture surface of concrete cone breakout which is a function of the loading direction and the relative position of edge/s w.r.t. the anchored rebars in tension.

The observed load–displacement response and crack patterns for the specimens (test and FE) are summarized in Fig. 7. Insights obtained from the measurements made during the tests that help to understand the characteristics of concrete breakout failure in each case are discussed for each specimen.

5.3.1 CH-25-DO: test results

The load displacement behavior and the crack pattern observed in the test and FE analysis for the specimen with a side edge loaded towards the edge are shown in Fig. 7a. The peak capacity in tests was observed to be lower in comparison to the FE results, with an



Table 2 Maximum load and displacement at the peak load measured in the experimental tests

Specimen	Peak load (kN)	Displacement @peak load (mm)	Rebar tension M (SG) (kN)	Rebar stress/ f_{yd} M (SG) (-)	Failure
CH-25-DO	35.95	22.96	137 (142.2)	64.2% (66.6%)	CC
CH-25-DI	38.65	26.76	149.1 (142.3)	69.9% (66.7)	CC
CH-25-DP	43.92	34.85	169.7 (175.5)	79.5% (82.2%)	CC
C25-25-DO	30.35	32.78	117.2 (83.8)	54.9% (54.9%)	CC

CC concrete cone

overestimation of the load of about 12%. This indicates that the FE modelling is affected by certain influences that play a crucial role in the present case. On the other side, the crack pattern in the FE analysis was found to be comparable to the test observations.

The failure of this this specimen is characterized with three distinct features:

- (i) Formation of a large breakout cone in the foundation region behind the column, as clearly shown by the crack pattern (Fig. 7a).
- (ii) Splitting tensile failure at the foundation edge location in the rebar end anchorage zone under the bending compression stresses from the column. This effect is evident in measured vertical crack widths using instruments (SWD and SWU, see Fig. 6a). A superposition of observed splitting tension crack widths plotted on a secondary scale with the load displacement curve is shown in Fig. 8a. An increase of splitting crack widths following the peak load can be clearly observed. This indicates that the splitting tensile failure at the foundation edge under the bending compression from the column played a significant role in the response in this case. It is likely that this effect was overestimated in the FE modelling approach.
- (iii) Concrete edge movements observed using instruments to measure crack width on the foundation top surface are shown in Fig. 8b. S-NA and S-SA represents sum total of the movements measured respectively at the north and south of the column, along the direction of load (i.e. sum of readings from the pair SNE-SNW and SSE-SSW respectively). S-ND and S-SD represent the crack

width in the diagonal direction at the north and south side of the column. It is observed that the relative movements of the foundation in vicinity of the column along the edge tended to stabilize in the post peak region. This indicates a rigid body translation of the entire rebar end anchorage zone, which was manifested in monotonically increasing diagonal movements which were observed to occur at the same time.

5.3.2 CH-25-DI: test results

The load displacement behavior and the crack pattern observed in the test and FE analysis for the specimen with a side edge loaded away from the edge are shown in Fig. 7b. The peak capacity in tests (offset = 25 mm) is greater (17%) compared to that evaluated in FE analysis (offset = 0 mm) as expected because of the relatively lower concrete strengths used in the analysis. The crack pattern observed in the tests was similar to that obtained from FE analysis.

The failure of this specimen was characterized by the following distinct features:

- (i) Local drop (kink) in the load displacement curve corresponding to the 1st crack in the diagonal direction (V shaped) at the foundation edge. The measured uplift at different location and the width of splitting cracks developing parallel to the tension reinforcement on the north and south side are presented in Fig. 9. It can be seen that the load drop corresponding to first crack coincides with a sudden increase in measured uplifts and the splitting crack widths.



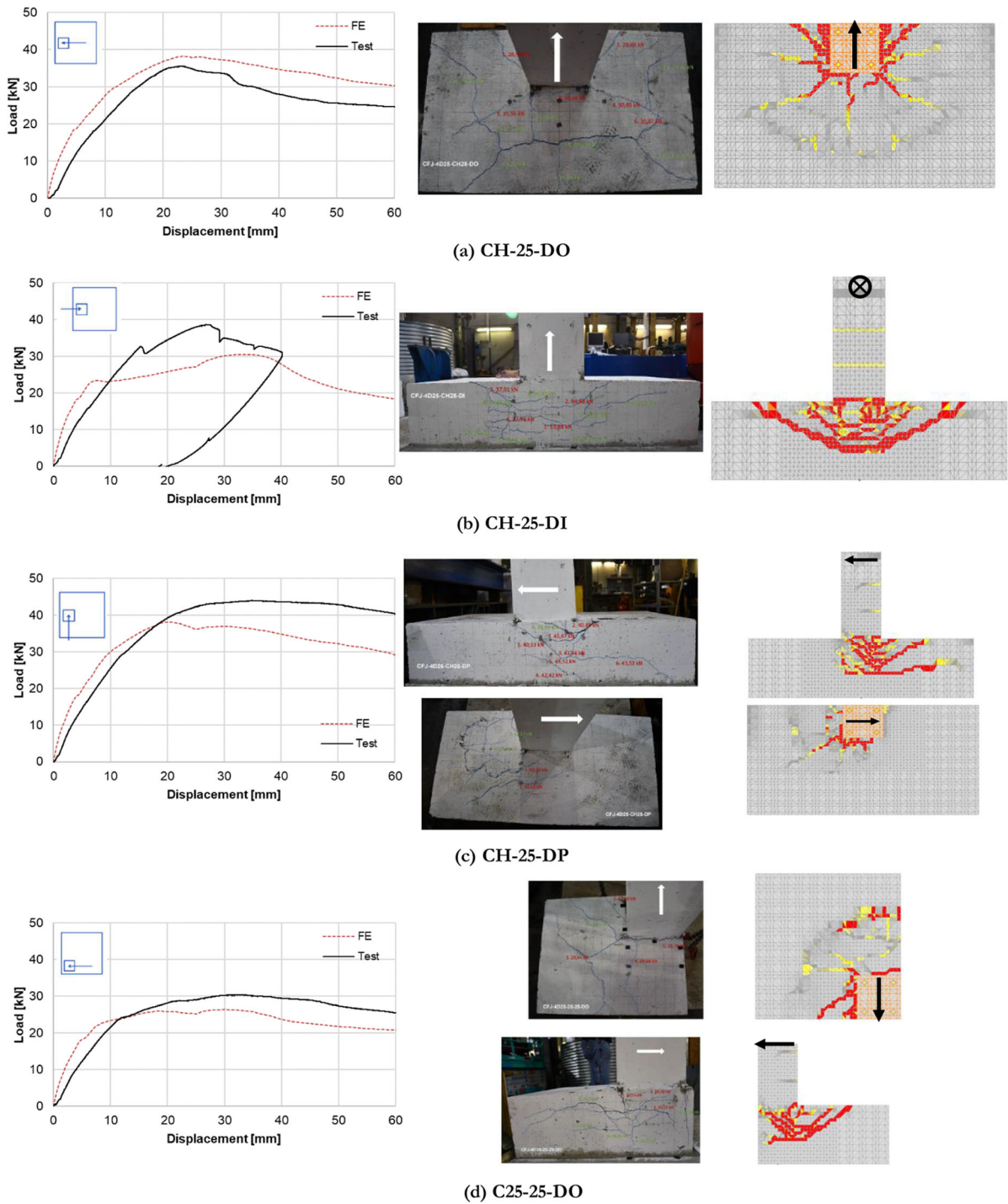


Fig. 7 Behavioral insights from tests and FE studies

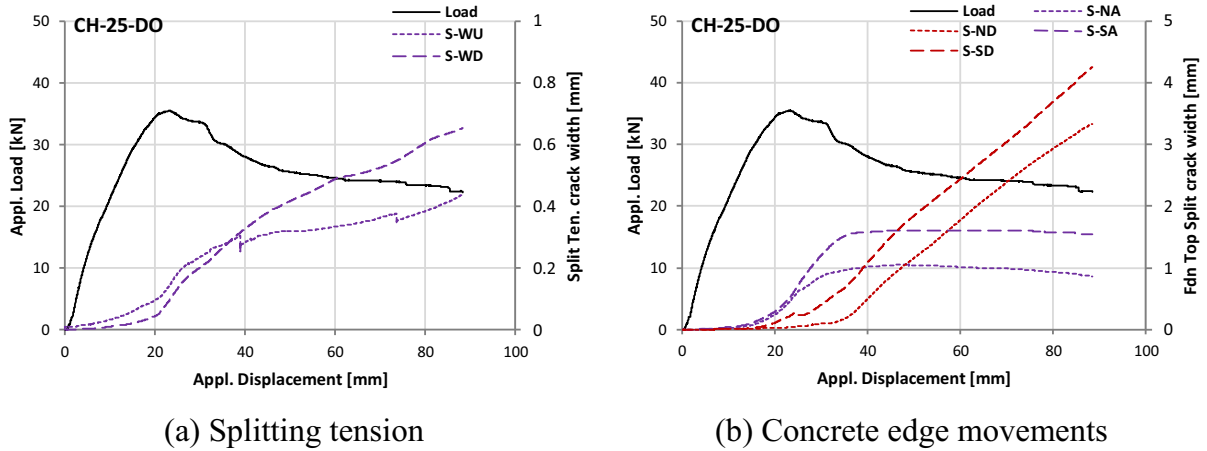


Fig. 8 Crack widths recorded during test on CH-25-DO

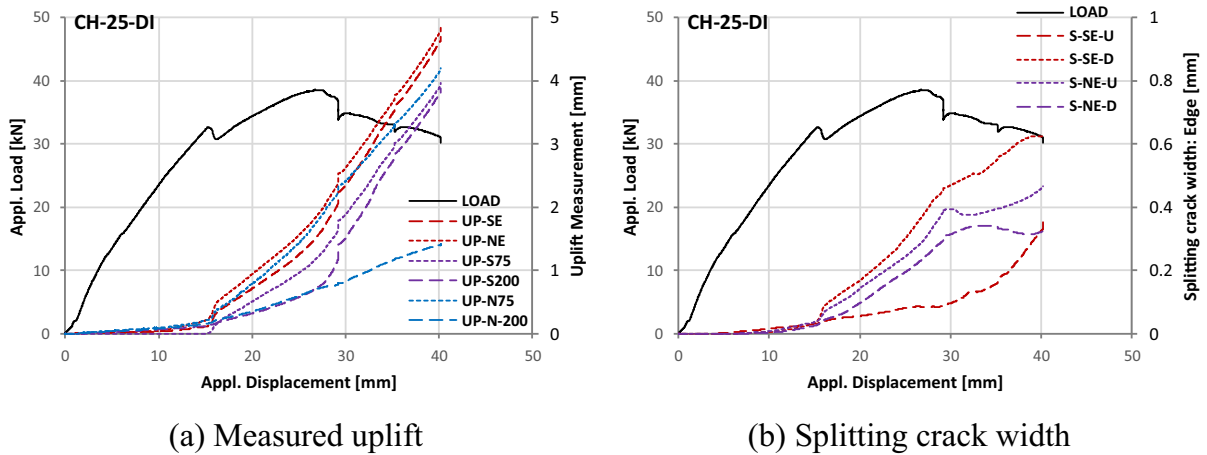


Fig. 9 Crack widths and uplift recorded during test on CH-25-DI

(ii) Stabilization of compression strut and its consequent failure: Following the 1st crack, the load increased, until the peak was reached after which the drop of load was relatively fast, accompanied by extensive damage at the foundation edge. This increase of load after 1st crack is attributed to the stabilization of the compressive strut between the anchored rebars in tension and the bending compression of column in the rebar end anchorage zone. At the peak load this strut failed and resulted in the sudden drop in the load. The stabilization and subsequent failure of

the strut was accompanied by increasing crack widths and uplifts as observed in Fig. 9.

5.3.3 CH-25-DP: test results

The load displacement behavior and the crack pattern observed in the test and FE analysis for specimen loaded parallel to the edge are shown in Fig. 7c. The experimental peak capacity (offset = 25 mm) was greater (9%) than that evaluated in FE analysis (offset = 0 mm). The crack pattern observed in the tests was similar to that obtained from FE analysis.



The failure of this specimen was characterized by the following distinct features:

- (i) Typical concrete cone formation cracks starting from the anchored end of the rebars were clearly visible. The diagonal crack representing splitting tension failure of the compression strut formed in the rebar anchorage zone was also clearly visible on the foundation edge.
- (ii) The initial damage prior to reaching the peak capacity was observed mainly on the edge of the foundation. In the post-peak region, the damage propagated into the inner region of the foundation. This is reflected better in the recorded crack width and rebar tension strain readings during the test as presented in Fig. 10. The primary radial crack through the plane containing the rebars manifested on the foundation edge as a vertical crack along the anchored tension rebar. The crack deviated at approximately 120° into the inside region of the foundation as seen in Fig. 7c. The corresponding crack widths (see Fig. 10a) were measured using S-SE-U and S-SE-D at the foundation edge (plotted as red curves) and using S-Di-100 and S-Di-250 (plotted with blue curve) in the inside region of the foundation. The strain in tension rebar located at the edge (in blue) and that located on the inside (in red) are presented in Fig. 10b. It is seen that the splitting crack widths at the edge tend to stabilize in the post peak region while those on

the inside show monotonic increase. Also the strain observed for the internal rebar follows the load–displacement curve closely in the post peak region. This clearly indicates a transfer of load carrying mechanism to the inside region of the foundation following the peak capacity.

5.3.4 C25-25-DO: test results

The load displacement behavior and the crack pattern observed in the test and FE analysis for the specimen with corner situation loaded towards the edge are shown in Fig. 7d. The peak capacity in tests (offset = 25 mm) was greater (5%) compared to that evaluated in FE analysis (offset = 0 mm). The crack pattern observed in the tests was comparable to that obtained from FE analysis.

The specimen represented a superposition of the cases CH-25-DO and CH-25-DP discussed in the previous sections. The characteristic features from the test CH-25-DO as well as CH-25-DP as discussed above were observed for this specimen. The failure in this case was characterized by a combination of (i) splitting tension failure in the anchorage zone region at the foundation edge right below the bending compression from the column, (ii) concrete edge movements in the direction of loading and (iii) developing of the splitting crack passing through the plane of tension rebars deviating at approximately 120° into the inside of the foundation which was

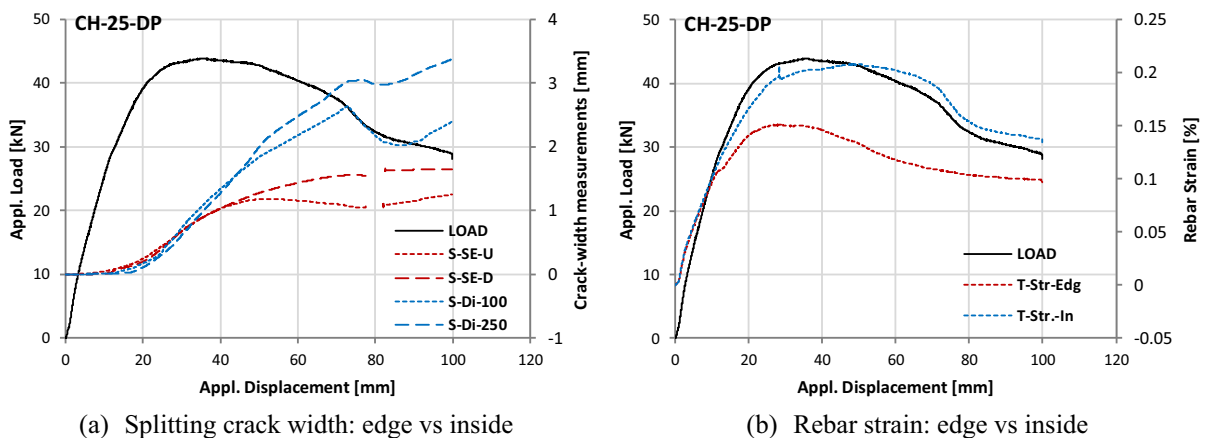


Fig. 10 Crack width and rebar strain recorded for CH-25-DP

responsible for transferring the load to the inner region of the foundation. Thus, the negative influences of the configuration CH-25-DO and the positive influences from CH-25-DP were combined in this special case.

6 Discussions in the light of concrete breakout theory

The objective of this research was to study the concrete breakout behavior in rebar end anchorage zones with edge proximity. It is noted here that in pre-test FE studies, an edge offset of 0 mm was used, while the same was 25 mm in tests. Furthermore, there is a slight difference in material properties of concrete evaluated in experiments ($f_{c,exp} = 17.9$ MPa and $f_{ct,exp} = 1.5$ MPa) and used in pre-test FE analysis ($f_{c,FE} = 20$ MPa and $f_{ct,FE} = 2.2$ MPa). In line with the expectations, the pre-test FE simulation are found to be underestimates (range of $\pm 15\%$) of the test results in all cases except for CH25-DO. For the case of CH25-DO, the capacity of localized concrete splitting failure under the bending compression load of the column was likely overestimated in the FE analysis leading to the observed discrepancy. Like the case with evaluation of FE results, the factor $\psi_{m,N}$ as applicable for the different tested cases are evaluated using (2). A summary of perspectives on the quantification of the factor $\psi_{m,N}$ is presented in Table 3. The factors $\psi_{m,N}$ derived from the FE simulations and the experiments are compared. In all cases, with the only exception of the reference specimen, the factor $\psi_{m,N} = 1.0$ is recommended by EOTA TR 069 [19] and EN 1992-4 [21]. However, as shown in Table 3, the numerical simulations as well as the experimental

results indicate that in general the concrete breakout resistance is increased by a factor $\psi_{m,N} \geq 1.0$ for most of the cases. It is interesting to observe that in the cases, where the concrete strut forming between the anchored end of tension rebars and the bending compression zone of the column is confined through continuity of foundation (i.e., cases CH-25-DI, CH-25-DP and C25-25-DI) the factor $\psi_{m,N}$ is at least of the same order of magnitude as for reference case (with no edge influence). The case CH-25-DO was observed to be an exception. The value of increasing factor $\psi_{m,N}$ is rather close to the unity. The case with outwards loading in the case of a side edge situation resulted in localized compressive stresses from column bending in the edge region. Because of the discontinuity in the foundation only limited confinement was available for the strut. This resulted in premature splitting tension failure in the localized region at the edge. Hence, beneficial effects of bending compression did not realize.

7 Concluding remarks

The objective of this paper was to discuss the benchmark experiments performed to obtain test data on behavioral perspectives on concrete breakout failure in column foundation joints subjected to proximity of foundation edge/s, which currently is not available. To this end FE studies were conducted on 6 cases which covered all possible edge proximity situations for column foundation joints. A total of 4 full scale experiments were conducted in this investigation. The main conclusions from the present study are summarized in the following points:

Table 3 Summarized insights on quantification of $\psi_{m,N}$: FE versus tests versus recommendation [19, 21]

ID	$\psi_{m,N}$ as per (2) from FE (-)	$\psi_{m,N}$ as per (2) from Exp (-)	Applicable $\psi_{m,N}$ [21] (-)	$\psi_{m,N,Exp}/\psi_{m,N,FE}$ (-)
CH-H-D (REF)	1.36	1.59	1.40	1.17
CH-25-DI	1.68	1.97	1.00	1.17
CH-25-DO	1.18	1.05	1.00	0.89
CH-25-DP	1.81	1.97	1.00	1.09
C25-25-DI	1.65	Not available	1.00	-
C25-25-DO	1.50	1.58	1.00	1.05



- FE analysis was used for the design and selection of specimens for testing in this paper. The comparison between FE pre-test analysis and experimental results shows that the adopted methodology of using FE analysis as a tool in combination with carefully selected benchmark experiments works in an efficient manner.
- Perspectives on the increasing factor applicable to concrete breakout resistance ($\psi_{m,N}$) which accounts for the effect of bending compression were obtained for different cases of edge proximity and loading directions. The case with a side edge and column loaded in an outwards direction (CH-25-DO) was found to provide worst influence of edge proximity. The value of increasing factor in this case was found to be equal to 1.0 (means no increasing factor). FE studies and recorded measurements revealed that this was primarily caused because the edge location negatively influenced the stability of the strut.
- In other cases of edge proximity (i.e., loading parallel to the edge or perpendicular away from the edge), the increasing factor evaluated from test and FE results were found to be on the same level to those provided by available expression of EN 1992-4. Therefore, in such cases the limitation of $\psi_{m,N} = 1.0$ leads to conservative capacity assessments.
- The results of PI anchorage presented in this paper are applicable to specific epoxy-based system employed in the present work and may not be generalized owing to product dependencies in case of PI adhesive systems. Additional investigations are required to generalize the conclusions of this study.
- In particular, the specimens investigated in this paper were designed to preclude all failure modes other than concrete breakout. In general, however, other failure modes (e.g. bond, rebar yielding) can govern the system response. At the system level, for the given material parameters and geometric configuration, all possible modes of failure are required to be compared and depending on the failure hierarchy [1, 20], the governing mode of failure and the system response can be estimated. To avoid failures in the anchorage zone and ensure ductile behaviour of the connections, it is desired that steel yielding is the governing failure mode in connection design.

Acknowledgements The authors extend their thanks to Hilti Corporation for providing the funding essential to conduct the tests presented in this paper. The support and suggestions provided Dr. Roberto Piccinin and Dr. Ulrich Bourgund during the course of this project is greatly appreciated by the authors. Opinions, conclusions and recommendations expressed in this paper are those of the authors, and do not necessarily reflect those of the funding organization.

Author contributions SC: Experimental Investigation, Writing-Original Draft, VM: Conceptualization, FE Investigation and specimen design, Writing-Original Draft, GG: Conceptualization, Writing-Original Draft, Supervision, Project administration, JH: Conceptualization, Writing-Review and Editing, Supervision, Project administration.

Funding Open Access funding enabled and organized by Projekt DEAL.

Open Access This article is licensed under a Creative Commons Attribution 4.0 International License, which permits use, sharing, adaptation, distribution and reproduction in any medium or format, as long as you give appropriate credit to the original author(s) and the source, provide a link to the Creative Commons licence, and indicate if changes were made. The images or other third party material in this article are included in the article's Creative Commons licence, unless indicated otherwise in a credit line to the material. If material is not included in the article's Creative Commons licence and your intended use is not permitted by statutory regulation or exceeds the permitted use, you will need to obtain permission directly from the copyright holder. To view a copy of this licence, visit <http://creativecommons.org/licenses/by/4.0/>.

References

1. Mahadik V (2022) Post installed rebar end anchorages in reinforced concrete connections. Ph.D. thesis, Institute of Construction Materials (IWB), University of Stuttgart, Germany
2. Haber ZB, Saiidi MS, Sanders DH (2014) Seismic performance of precast columns with mechanically spliced column-footing connections. *ACI Struct J* 111(3):639–650
3. Nascimbene R, Bianco L (2021) Cyclic response of column to foundation connections of reinforced concrete precast structures: numerical and experimental comparisons. *Eng Struct* 247:113214
4. Yuan H, Zhenggeng Z, Naito CJ, Weijian Y (2017) Tensile behavior of half grouted sleeve connections: experimental study and analytical modeling. *Constr Build Mater* 152:96–104
5. Popa V, Papurcu A, Cotofana D, Pascu R (2015) Experimental testing on emulative connections for precast columns using grouted corrugated steel sleeves. *Bull Earthq Eng* 13:2429–2447
6. Genesio G (2012) Seismic assessment of RC exterior beam-column joints retrofitted with haunches using post-installed



- anchors. Ph.D. thesis, Institut für Werkstoffe im Bauwesen, Universität Stuttgart
7. Metelli G, Messali F, Beschi C, Riva P (2015) A model for beam-column corner joints of existing RC frame subjected to cyclic loading. *Eng Struct* 89:79–92
 8. Mahadik V, Sharma A, Hofmann J (2020) Re-evaluation of existing tests on RC connections using post-installed reinforcing bars. *Eng Struct* 209:109970
 9. Cattaneo S, Genesio G, Piccinin R (2020) Design of anchorages in connections using post-installed reinforcing bars. In: Italian concrete days
 10. Tanaka R, Oba K (2001) Experimental study on seismic performance of beam members connected with post-installed anchors. In: Proceedings of the symposium on connections between steel and concrete, Stuttgart, Germany, pp 576–85
 11. Kupfer H, Munger F, Kunz J, Jahring A (2003) Hauptaufsatze-Nachtraglich verankerte gerade Bewehrungsstäbe bei Rahmenknoten (Anchorage of post installed straight bars for frame node connections). *Bauingenieur* 78(1):24–37
 12. Hamad BS, Al Hammoud R, Kunz J (2006) Evaluation of bond strength of bonded-in or post-installed reinforcement. *ACI Struct J* 103(2):207–218
 13. Mahrenholtz C (2012) Seismic bond model for concrete reinforcement and the application to column-to-foundation connections. Ph.D. thesis, Institut für Werkstoffe im Bauwesen, Universität Stuttgart, Germany
 14. Mahrenholtz C, Akguzel U, Eligehausen R, Pampanin S (2014) New design methodology for seismic column-to-foundation anchorage connections. *ACI Struct J* 111(5):1179–1189
 15. Herzog MB (2015) Contribution on the harmonization of design in reinforced concrete construction and fastening technology. Ph.D. thesis, Institut für Werkstoffe im Bauwesen, Universität Stuttgart (**in German**)
 16. Mahadik V, Sharma A, Hofmann J (2018) Seismic performance of column-foundation-joints with post-installed rebar connections: pre-test simulations. In: High tech concrete: where technology and engineering meet. Springer, pp 1033–40
 17. Mahadik V, Sharma A, Hofmann J (2021) Cast-in and post-installed rebar anchorage systems in RC column foundation joints: experimental investigations. *Eng Struct* 238:112
 18. EAD-332402 (2019) Post-Installed reinforcing bar (Rebar) connections with improved bond-splitting behaviour under static loading. European Organization for Technical Assessment (EOTA), European Assessment Document EAD 332402-00-0601
 19. TR-069 (2019) Design method for anchorage of post-installed reinforcing bars (rebars) with improved bond-splitting behavior as compared to EN 1992-1-1. European Organization for Technical Assessment (EOTA)
 20. Mahadik V, Sharma A, Hofmann J (2023) Cast-in and post-installed rebar anchorage systems in RC column foundation joints: system specific assessment and design. *Eng Struct* 276:115356s
 21. EN:1992-4 (2018) Eurocode 2—design of concrete structures—part 4: design of fastenings for use in concrete. British Standard Institutions (BSI)
 22. Mahadik V, Hofmann J, Genesio G, Sharma A (2022) Concrete breakout failures in rebar end anchorage zones. In: Proceedings of 5th conference on bond in concrete, Stuttgart
 23. Hofmann J, Mahadik V, Sharma A (2022) Assessment framework in background of TR069. In: Proceedings of 5th conference on bond in concrete, Stuttgart
 24. Mahrenholtz C, Eligehausen R, Reinhardt H-W (2020) Qualification and design of cast-in-place and post-installed reinforcing bar anchorages. *ACI Struct J* 117(2):3–16
 25. Mahrenholtz C, Eligehausen R, Reinhardt H-W (2015) Design of post-installed reinforcing bars as end anchorage or as bonded anchor. *Eng Struct* 100:645–655
 26. Fuchs W, Eligehausen R, Breen JE (1995) Concrete capacity design (CCD) approach for fastening to concrete. *Struct J* 92(1):73–94
 27. Eligehausen R, Mallee R, Silva JF (2006) Anchorage in concrete construction. Wiley, New York
 28. ACI-318-19 (2019) Building code requirements for structural concrete (ACI 318-19) and commentary (ACI 318R-19). American Concrete Institute
 29. FEMAP (2015) Finite element modelling and postprocessing (FEMAP v11.2). Siemens Industry Software Inc
 30. Ozbolt J (2010) Masa 3: finite element program for 3D nonlinear analysis of concrete and reinforced concrete structures
 31. Ozbolt J, Li Y, Kozar I (2001) Microplane model for concrete with relaxed kinematic constraint. *Int J Solids Struct* 38(16):2683–2711

Publisher's Note Springer Nature remains neutral with regard to jurisdictional claims in published maps and institutional affiliations.

